ond, the quantity of medical information displayed on the screen of IEMAS was not considered adequate by the operating surgeon in some cases. Therefore, the device was improved by modifications. The details of its initial clinical testing was reported previously and published elsewhere.[21] Here we present our clinical experience with routine use.

Materials and Methods

IEMAS was designed as an information-sharing device for use during awake craniotomy for intracranial lesions.[6] The device provides simultaneous real-time visualization of a wide spectrum of intraoperative data. For example, the patient's mimic and face movements during answering specific test questions, type of the examination test, position of the surgical instruments and cortical stimulator in the surgical field, parameters of the bispectral index monitor, and general view of the surgical field through the operating microscope, can be presented compactly in one screen with several displays (Fig. 1). Moreover, this combined image can be projected on several in-room liquid crystal display (LCD) monitors, so the integrated real-time information can be easily distributed and quickly analyzed by all members of the surgical team, practically without interruption of the surgical manipulations.

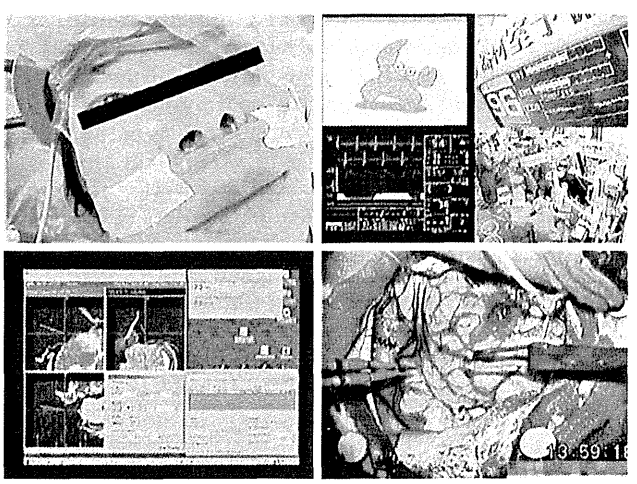

Fig. 1 Integration of multiple intraoperative parameters on the screen of the wireless intraoperative examination monitor for awake surgery. On the *upper left* display, the patient face and eyes can be seen to facilitate checking of the consciousness status and mimics during response to test questions. On the *lower left* display, the anatomical data from the real-time updated neuronavigation system is shown, which can localize the exact position of the cortical stimulator. On the *lower right* display, the view of the surgical field through the operative microscope during brain mapping is seen, which can be helpful for precise identification of the timing of stimulation. On the *upper right* display, 4 different types of information are presented, which are (*clockwise*): the test object provided for a patient for naming, parameters of the bispectral index monitor reflecting the patient's awake state, general view of the operating theater, and parameters of the heart beat monitor. In total, 7 different intraoperative parameters are integrated in real-time on one screen.

The specific feature of the new modification of the IEMAS system is the installation of wireless information transmitting technology using audio-visual transmitters and receivers for transfer of images and verbal information.[21] The general technical characteristics are presented in Table 1. The device consists of 3 main parts: patient monitor, operator monitor, and control box (Fig. 2).

The patient monitor is a 3.5-inch LCD with a small

Table 1 Technical parameters of the latest modification of intraoperative examination monitor for awake surgery

Size (mm)	390 × 1100 × 1300
Power supply (V)	AC 100; DC 12
Frequency range of audio-visual transmitters	1.2 GHz (1 channel) and 2.45 GHz (2 channels)
Camera and monitors	CCD camera 3.5 inch LCD monitor (patient monitor) 7.5 inch LCD monitor (operator monitor)
Degrees of freedom in monitors positioning	6 (self-controlling)

AC: alternating current, CCD: charge coupled device, DC: direct current, LCD: liquid crystal display.

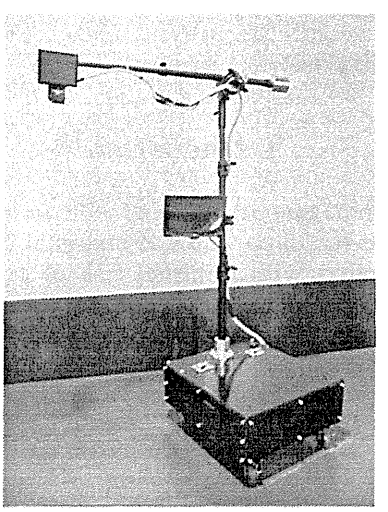

Fig. 2 General view of the wireless modification of intraoperative examination monitor for awake surgery. Three main parts of the device are seen, patient monitor, operator monitor, and control box.

charge coupled device (CCD) camera and incorporated highly sensitive microphone. The test questions for the patient are displayed on this monitor, and the camera images the patient's face simultaneously with the verbal response to tests. The operator monitor is a 7.5-inch LCD, which can project various intraoperative parameters. The whole combined image is constructed with a special divider of the recording system. In the modified IEMAS, 7 separate windows can be created on this screen, compared with 5 on the previous version of the device. The image of this monitor is recorded on the hard disk of the recording system, which is located outside the operating room (Fig. 3). The control box contains a down scan converter, alternating current power supply, and audio-visual transmitters and receivers. Metal poles connecting all 3 components of the device are made from the recreated parts of the commercially available tripod.

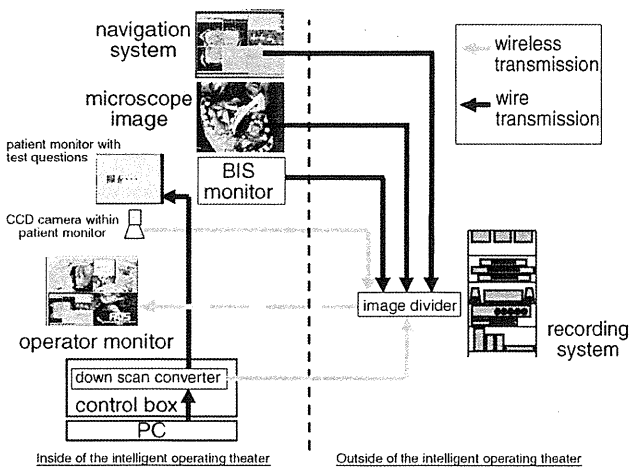

Fig. 3 Scheme of information transfer during use of intraoperative examination monitor for awake surgery and signal exchanging system provided by audio-visual transmitters and receivers. BIS: bispectral index, CCD: charge coupled device, PC: personal computer.

In the operating theater, the compact device is located beside the operating table and controlled by the assistant in charge of brain function monitoring (Fig. 4), whose main tasks include providing of the test questions for the patient simultaneously with electrical stimulation of the cerebral cortex performed by the operating surgeon, and checking the appropriateness of response by evaluation of both the verbal answer and movements of the facial muscles and eyeballs.

Results

A total of 939 neurosurgical procedures for resection of intracranial gliomas were performed in the intelligent operating theater of the Tokyo Women's Medical University from March 2000 to January 2011. Awake craniotomy was performed in 220 cases, and the initial modification of IEMAS was used 186 times.

The clinical testing of the new modification of the device was initiated on February 1, 2010, and immediately revealed the presence of crossed line effects, which resulted in impaired quality of visual and auditory data. This technical trouble was caused by imperfect design of the control box, with close vicinity of the several transmitters and receivers within the same tight space, as well as by use of a similar frequency (2.4 GHz) for all transmitters. Change of the

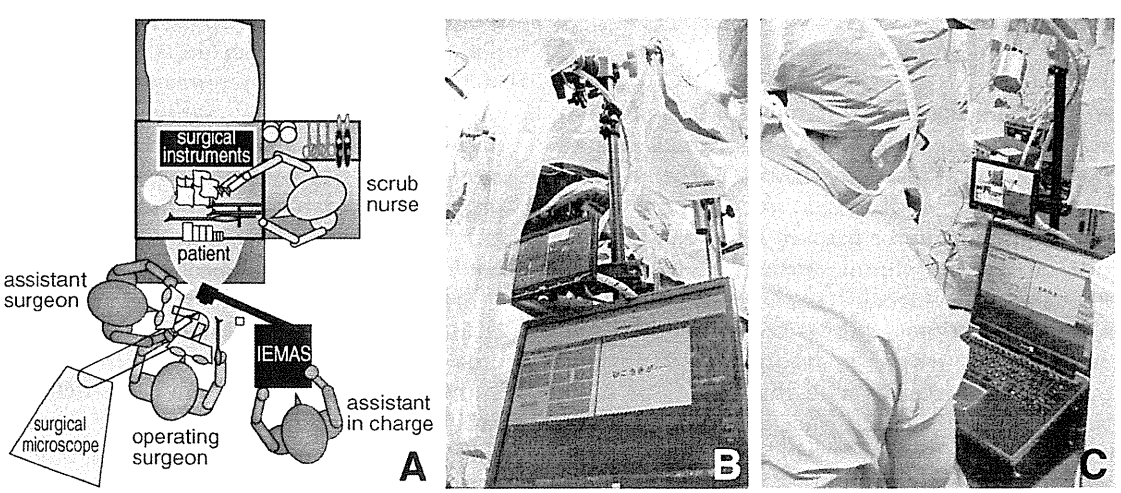

Fig. 4 Schematic (A) and real (B) demonstration of the position of the intraoperative examination monitor for awake surgery (IEMAS) during resection of glioma, and its use by the assistant in charge of brain mapping (C).

Table 2 Possible problems with identification of the speech areas with intraoperative electrical stimulation of the cerebral cortex during awake craniotomy and technical solutions required for their elimination*

Problem	Solution
Speech arrest during intraoperative cortical mapping may be similarly caused by stimulation of the different cortical areas, namely motor cortex, negative motor cortex, and speech area itself, which requires their precise discrimination. Presence of the surgical drapes separating the patient face and examination monitor from the examiner of the cortical functions may result in problems with identification of important neurological signs appearing during cortical stimulation, and with assessment of the appropriateness of visualization of the examination task by the patient.	Monitoring of the patient face, its mimics, and involuntary movements of the facial muscles at the time of speech arrest during cortical stimulation may be extremely helpful for ruling out both false positive and false negative identification of the speech area and for its precise localization.
Insufficient awakening of the patient from sedation and suboptimal level of his or her conscious may result in poor response to examination tasks and pseudo speech arrest, which may result in false positive identification of the cortical speech area.	Information on the patient sedation level should be integrated with details of his or her response to the examination tasks and those data should be provided both for the surgeon and examiner of the cortical functions.
It may be difficult for the surgeon to assess correctness of the patient response to examination task, since at the same time he or she performs electrical stimulation of the cortex. The examiner of the cortical functions providing the examination tasks for the patient cannot see the nuances of the cortical stimulation performed by the surgeon, which may create problems with precise interpretation of the patient responses.	The information on the cortical stimulation observed by the surgeon through the operating microscope and data on the type of examination task providing for the patient and his or her response should be integrated in real-time. Moreover, this information should be preferably provided not only for the surgeon and examiner of the cortical functions, but for all other members of the surgical team in order to prevent loss of the important information and its correct interpretation.
Even if according to the intraoperative cortical mapping it can be suspected that speech area is localized correctly, it may be difficult for a surgeon to integrate precisely its positioning with the anatomical details of the tumor location.	The information on the electrical cortical stimulation during intraoperative brain mapping should be integrated with the data of intraoperative neuronavigation with three-dimensional visualization of the tumor location.

*According to Yoshimitsu et al.[21] and Sakurai et al.[19]

wireless connections between the image divider and operator monitor to cables was successfully done initially,[21] but simple reduction of the frequency of this transmitter from 2.4 GHz to 1.2 GHz was soon found to be adequate for full resolution of the problem. The wireless modification of IEMAS was used during 34 subsequent awake craniotomies without technical problems during the 12 subsequent months.

Discussion

Precise intraoperative localization of the eloquent cortical areas is of paramount importance during resection of cerebral gliomas. However, the anatomical location has individual variations.[13-15,17,18] Moreover, indolent tumor growth may result in further shift of the functional cortical centers away from the mass. Therefore, intraoperative mapping of cortical and, sometimes, subcortical cerebral structures is essential, which is frequently performed during awake craniotomy with the conscious communicating patient during direct electrical stimulation of the specific brain areas.[1,3,8-10,16,20] Several problems may arise with identification of the cortical speech areas using such technique and require specific solutions (Table 2).[19,21] Particularly, elimination of the anarthria produced by positive motor response of the tongue and face or from the negative motor response of the tongue during cortical stimulation is extremely important for precise evaluation of the language function.[2,10]

Our IEMAS may significantly facilitate cortical brain mapping during awake craniotomy and definitely proved its usefulness.[5,6,11,19] However, sometimes appropriate use suffered from occasional interruption of the connecting cables or detachment. Moreover, the operating surgeon had complained on several occasions of the limited number of intraoperative parameters visualized on the screen of the monitor. While those problems were definitely minor, anxiety and irritation can result for members of the surgical team due to more or less prolonged interruption of the tumor removal. The latter is definitely highly undesirable taking into account the awake condition of the patient.

Modification of the device was directed on installation of the wireless transmitting functions and increase of the number of windows on the operator monitor screen. Some technical problems appearing during initial clinical testing were resolved quickly. Our experience with the modified IEMAS suggests complete elimination of minor problems associated with the previous version. The compact and wireless structure is very convenient to use in the narrow space of the operating room. Further efforts with im-

provement of the IEMAS will include development of a more comfortable user interface and installation of the auto-tracking mechanism in the CCD camera of the patient monitor for automatic correction of its positioning during cortical mapping.

Acknowledgment

These data were presented in part during 32nd Annual International Conference of the IEEE Engineering in Medicine and Biology Society "Merging Medical Humanism and Technology" (August 31-September 4, 2010; Buenos Aires, Argentina).

References

1) Bello L, Galucci M, Fava M, Carrabba G, Giussani C, Acerbi F, Baratta P, Songa V, Conte V, Branca V, Stocchetti N, Papagno C, Gaini SM: Intraoperative subcortical language tract mapping guides surgical removal of gliomas involving speech areas. *Neurosurgery* 60: 67-82, 2007
2) Duffau H: Contribution of cortical and subcortical electrostimulation in brain glioma surgery: methodological and functional considerations. *Neurophysiol Clin* 37: 373-382, 2007
3) Duffau H, Capelle L, Denvil D, Sichez N, Gatignol P, Taillandier L, Lopes M, Mitchell MC, Roche S, Muller JC, Bitar A, Sichez JP, van Effenterre R: Usefulness of intraoperative electrical subcortical mapping during surgery for low-grade gliomas located within eloquent brain regions: functional results in a consecutive series of 103 patients. *J Neurosurg* 98: 764-778, 2003
4) Iseki H, Muragaki Y, Nakamura R, Ozawa N, Taniguchi H, Hori T, Takakura K: Intelligent operating theater using intraoperative open-MRI. *Magn Reson Med Sci* 4: 129-136, 2005
5) Iseki H, Nakamura R, Muragaki Y, Suzuki T, Chernov M, Hori T, Takakura K: Advanced computer-aided intraoperative technologies for information-guided surgical management of gliomas: Tokyo Women's Medical University experience. *Minim Invasive Neurosurg* 51: 285-291, 2008
6) Iseki H, Nambu K: [Intraoperative Examination Monitoring for Awake Surgery (IEMAS)]. *No Shinkei Geka* 33: 1028-1031, 2005 (Japanese)
7) Kayama T, Kumabe T, Tominaga T, Yoshimoto T: Prognostic value of complete response after the initial treatment for malignant astrocytoma. *Neurol Res* 18: 321-324, 1996
8) Kayama T, Sato S: [Definition of individual language related area by awake surgery]. *No To Shinkei* 53: 151-160, 2001 (Japanese)
9) Kim SS, McCutcheon IE, Suki D, Weinberg JS, Sawaya R, Lang FF, Ferson D, Heimberger AB, DeMonte F, Prabhu SS: Awake craniotomy for brain tumors near eloquent cortex: correlation of intraoperative cortical mapping with neurological outcomes in 309 consecutive patients. *Neurosurgery* 64: 836-846, 2009
10) Mikuni N, Miyamoto S: Surgical treatment for glioma: extent of resection applying functional neurosurgery. *Neurol Med Chir (Tokyo)* 50: 720-726, 2010
11) Muragaki Y, Iseki H, Maruyama T, Kawamata T, Yamane F, Nakamura R, Kubo O, Takakura K, Hori T: Usefulness of intraoperative magnetic resonance imaging for glioma surgery. *Acta Neurochir Suppl* 98: 67-75, 2006
12) Muragaki Y, Iseki H, Maruyama T, Tanaka M, Shinohara C, Suzuki T, Yoshimitsu K, Ikuta S, Hayashi M, Chernov M, Hori T, Okada Y, Takakura K: Information-guided surgical management of gliomas using low-field-strength intraoperative MRI. *Acta Neurochir Suppl* 109: 67-72, 2011
13) Ojemann G, Ojemann J, Lettich E, Berger M: Cortical language localization in left, dominant hemisphere. An electrical stimulation mapping investigation in 117 patients. *J Neurosurg* 71: 316-326, 1989
14) Ojemann GA: Neurosurgical management of epilepsy: a personal perspective in 1983. *Appl Neurophysiol* 46: 11-18, 1983
15) Ojemann JG, Miller JW, Silbergeld DL: Preserved function in brain invaded by tumor. *Neurosurgery* 39: 253-259, 1996
16) Otani N, Bjeljac M, Muroi C, Weniger D, Khan N, Wieser HG, Curcic M, Yonekawa T: Awake surgery for glioma resection in eloquent areas: Zurich's experience and review. *Neurol Med Chir (Tokyo)* 45: 501-511, 2005
17) Pouratian N, Cannerstra AF, Bookheimer SY, Martin NA, Toga AW: Variability of intraoperative electrocortical stimulation mapping parameters across and within individuals. *J Neurosurg* 101: 458-466, 2004
18) Quinones-Hinojosa A, Ojemann SG, Sanai N, Dillon WP, Berger MS: Preoperative correlation of intraoperative cortical mapping with magnetic resonance imaging landmarks to predict localization of the Broca area. *J Neurosurg* 99: 311-318, 2003
19) Sakurai Y, Muragaki Y, Okada Y, Nambu K, Iseki H: The development and application of the device for intraoperative examination monitor for awake surgery. *Journal of Tokyo Women's Medical University* 81: 32-40, 2011
20) Sanai N, Mirzadeh Z, Berger MS: Functional outcome after language mapping for glioma resection. *N Engl J Med* 358: 18-27, 2008
21) Yoshimitsu K, Suzuki T, Muragaki Y, Chernov M, Iseki H: Development of modified intraoperative examination monitor for awake surgery (IEMAS) system for awake craniotomy during brain tumor resection. *Conf Proc IEEE Eng Med Biol Soc* 2010: 6050-6053, 2010

Address reprint requests to: Kitaro Yoshimitsu, PhD, Faculty of Advanced Techno-Surgery, Institute of Advanced Biomedical Engineering and Science, Tokyo Women's Medical University, 8-1 Kawada-cho, Shinjuku-ku, Tokyo 162-8666, Japan.
e-mail: kitaro@abmes.twmu.ac.jp

INTERNATIONAL JOURNAL OF
UROLOGY
International Journal of Urology (2013) 20, 993–999 doi: 10.1111/iju.12091

Original Article: Clinical Investigation

Ability of preoperative 3.0-Tesla magnetic resonance imaging to predict the absence of side-specific extracapsular extension of prostate cancer

Tomohiko Hara,[1] Hiroyuki Nakanishi,[1] Tohru Nakagawa,[1] Motokiyo Komiyama,[1] Takashi Kawahara,[1] Tomoko Manabe,[2] Mototaka Miyake,[2] Eri Arai,[3] Yae Kanai[3] and Hiroyuki Fujimoto[1]

[1]Urology Division, National Cancer Center Hospital, [2]Diagnostic Radiology Division, National Cancer Center Hospital, and [3]Division of Molecular Pathology, National Cancer Center Research Institute, Tokyo, Japan

Abbreviations & Acronyms
3.0-T = 3.0-Tesla
ADC = apparent diffusion coefficient
CI = confidence interval
DRE = digital rectal examination
DWI = diffusion-weighted imaging
ECE = extracapsular extension
MRI = magnetic resonance imaging
NPV = negative predictive value
OR = odds ratio
PPV = positive predictive value
PSA = prostate-specific antigen
PZ = peripheral zone
RP = radical prostatectomy
T = Tesla
T2WI = T2-weighted imaging
TRUS = transrectal ultrasonography
TZ = transitional zone

Correspondence: Tomohiko Hara M.D., Ph.D., Urology Division, National Cancer Center Hospital, Tsukiji 5-1-1, Chuo-ku, Tokyo 104-0045, Japan. Email: tomohara-jua@umin.ac.jp

Received 15 August 2012; accepted 26 December 2012. Online publication 29 January 2013

Objective: Recent studies have shown an improvement in prostate cancer diagnosis with the use of 3.0-Tesla magnetic resonance imaging. We retrospectively assessed the ability of this imaging technique to predict side-specific extracapsular extension of prostate cancer.

Methods: From October 2007 to August 2011, prostatectomy was carried out in 396 patients after preoperative 3.0-Tesla magnetic resonance imaging. Among these, 132 (primary sample) and 134 patients (validation sample) underwent 12-core prostate biopsy at the National Cancer Center Hospital of Tokyo, Japan, and at other institutions, respectively. In the primary dataset, univariate and multivariate analyses were carried out to predict side-specific extracapsular extension using variables determined preoperatively, including 3.0-Tesla magnetic resonance imaging findings (T2-weighted and diffusion-weighted imaging). A prediction model was then constructed and applied to the validation study sample.

Results: Multivariate analysis identified four significant independent predictors ($P < 0.05$), including a biopsy Gleason score of ≥8, positive 3.0-Tesla diffusion-weighted magnetic resonance imaging findings, ≥2 positive biopsy cores on each side and a maximum percentage of positive cores ≥31% on each side. The negative predictive value was 93.9% in the combination model with these four predictors, meanwhile the positive predictive value was 33.8%. Good reproducibility of these four significant predictors and the combination model was observed in the validation study sample.

Conclusions: The side-specific extracapsular extension prediction by the biopsy Gleason score and factors associated with tumor location, including a positive 3.0-Tesla diffusion-weighted magnetic resonance imaging finding, have a high negative predictive value, but a low positive predictive value.

Key words: 3.0-Tesla diffusion-weighted magnetic resonance imaging, capsular invasion, extracapsular extension, nerve-sparing radical prostatectomy, prostate cancer.

Introduction

MRI has considerable potential to improve the accuracy of prostate cancer diagnosis.[1] DWI in MRI is a non-invasive technique that provides information about cell density and diffusion restriction in cancerous tissue.[2] Recent studies have shown improved diagnostic accuracy with the combined use of 3.0-T DWI MRI and T2WI MRI for patients with prostate cancer.[3,4]

ECE of prostate cancer is an important predictor of the outcome of RP.[5,6] Many urologists have attempted to predict ECE location using various preoperative parameters, such as clinical stage, Gleason score and preoperative serum PSA level.[5,7,8] However, the preoperative diagnostic accuracy using these conventional parameters is limited. Therefore, we hypothesized that 3.0-T MRI information combined with conventional preoperative features might facilitate more accurate prediction of side-specific ECE.

Methods

Patient population

From October 2007 to August 2011, open retropubic radical prostatectomy after preoperative 3.0-T MRI examination was carried out in 396 patients at the National Cancer Center Hospital of Tokyo, Japan. Of these, 130 were excluded because they received neoadjuvant therapy, provided insufficient data for analysis or were diagnosed with tumors other than adenocarcinoma. Of the remaining patients, 132 patients who were diagnosed with T1c–T3a prostate cancer after undergoing 12-core prostate biopsy at our institution were enrolled as a primary study sample. Systematic 12-core biopsy specimens were obtained under the guidance of TRUS using an end-fire probe (B-K Medical, Herlev, Denmark). Meanwhile, a validation study sample including 134 patients who had undergone ≥10 core biopsies at other institutions was enrolled. Results of all biopsies were reviewed by two pathologists (EA and YK).

Pathological evaluation

All biopsy samples and resected specimens were evaluated by two pathologists (EA and YK). The Gleason score was obtained by summing the primary and secondary tumor grades. In our institution, the location and Gleason scores for 12 biopsy cores are recorded as a systematic part of the biopsy process. For both sides in all patients, the number and maximum percentage of positive biopsy cores were calculated. For side-specific evaluation of the specimens, the prostates were visually divided bilaterally (right and left sides). Then the extent of side-specific prostatic capsular invasion on each side was measured. Results were divided into two categories: ECE side and non-ECE side (i.e. side with no cancer focus). The non-ECE side was subclassified into a capsular contact side, in which the tumor was confined to the prostate within a layer more fibrous than muscular (capsule),[9] and a non-capsular contact or no cancer side.

Clinical cancer staging and evaluation of prostatic capsular invasion levels

Cancer stage was assigned on the basis of the 2009 Union for International Cancer Control 7th TNM staging system.[10] Conventional T1/T2WI and DWI MRI was carried out using a clinical 3.0-T MRI system (Magnetom Trio with TIM system; Siemens, Erlangen, Germany) and a standard body coil. *B*-values of DWI were 0–1500 s/mm^2. MRI was carried out preoperatively over a period of 4 weeks after biopsy. MRI images were preoperatively assessed by two radiologists (TM and MM). The findings of T2WI were evaluated for cancer location and visually categorized as follows: unremarkable, organ-confined cancer without capsular contact, cancer with capsular contact and ECE cancer. A cancer focus with ECE on T2WI MRI was defined as T2WI MRI-positive. The slice thickness of our 3.0-T MRI T2WI was 0.73 mm. Therefore, the detection of microscopic ECE (<1 mm) was difficult using MRI. We referenced the previously reported criteria to predict the microscopic ECE by MRI findings, which consisted of the disruption of the prostatic capsule, extension into the periprostatic fat, broad contact with the capsule (>12 mm), irregular capsular bulge, obliteration of the rectoprostatic angle and neurovascular bundle involvement.[11] The findings of DWI MRI were visually categorized as follows: unremarkable, confined to the prostate without capsular contact and capsular contact or ECE cancer. The last was a dual category, because it was difficult to clearly distinguish the ECE side with DWI MRI alone. A cancer focus with capsular contact or ECE on DWI MRI was defined as DWI MRI-positive. When evaluation of cancer location was difficult because of residual bleeding caused by biopsy or measurement artifacts, MRI T2WI and DWI findings were judged to be unremarkable. Clinical TNM staging was determined using a combination of DRE, TRUS and MRI information.

Methods of analysis

In the primary study sample, the association of side-specific ECE with clinical and biopsy features was assessed using the Wilcoxon rank-sum test with continuity correction and Fisher's exact test. The variables, including serum PSA level, biopsy Gleason score, DRE, TRUS, the number of positive biopsy cores on each side, the maximum percentage of positive cores on each side, T2WI MRI findings, and DWI MRI findings were tested using univariate and multivariate logistic regression analyses to evaluate their association with side-specific ECE. The optimal cut-off values maximizing the sum of sensitivity plus specificity were statistically determined for the univariate analyses. Multivariate logistic regression analyses used backward, stepwise selection for variables with $P < 0.1$ in the univariate analyses, and the variable remained if the significance level was $P < 0.05$ for that variable. Statistically significant factors ($P < 0.05$) according to multivariate logistic regression analysis were used to construct a model for the prediction of side-specific ECE. The predictive accuracy for the model was quantified by measuring sensitivity, specificity, PPV, NPV, diagnostic accuracy and OR. The accuracy of the constructed prediction model for the determination of side-specific ECE was validated using the validation study sample. A flowchart was then constructed on the basis of the prediction model for both study samples. All statistical analyses were carried out using the freely downloadable *R* statistical software v2.13.0 (http://cran.r-project.org).[12]

Results

Bilateral and unilateral nerve-sparing RP was carried out in four (3.0%) and 18 (13.6%) of the 132 patients in the

Table 1 Clinical and pathological characteristics in the primary and validation study samples

	Primary study set (132 patients)	Validation study set (134 patients)
Variables		
Median age, years (range)	65.5 (51–78)	65 (50–81)
Median serum PSA value (range)	8.5 (2.2–67.0)	7.9 (3.3–57.9)
Biopsy Gleason score; *n* (%)		
6 or less	10 (7.6)	9 (6.7)
3 + 4	59 (44.7)	52 (38.8)
4 + 3	49 (37.1)	53 (39.6)
8 or greater	14 (10.6)	20 (14.9)
Clinical T stage; *n* (%)		
T1c	9 (6.8)	12 (9.0)
T2a/b	44 (33.3)	65 (48.5)
T2c	37 (28.0)	28 (20.9)
T3a	42 (31.8)	29 (21.6)
Pathological T stage; *n* (%)		
pT2a/b	22 (16.7)	24 (17.9)
pT2c	48 (36.4)	57 (42.5)
pT3a	47 (35.6)	43 (32.1)
pT3b	15 (11.4)	10 (7.5)
Pathological capsular invasion extent in each lobe		
Non-ECE		
No capsular contact + no cancer focus	62 (23.5)	67 (25.0)
Capsular contact	131 (49.6)	140 (52.2)
ECE	71 (26.9)	61 (22.8)

primary sample, and two (1.5%) and 25 (18.7%) of the 134 patients in the validation sample, respectively. All surgical margins were negative on the nerve-sparing sides. Therefore, these sides were included in the analysis. The clinical and pathological features of the study samples are shown in Table 1. Neither positive imaging nor significant DRE findings were found in nine (6.8%) and 12 (9.0%) of the T1c patients in the primary and validation samples, respectively. The well-developed and extended prostatectomy technique used in our institution was used for all high-risk and relatively high-risk patients.[13] Therefore, pathologically confirmed side-specific ECE cancer was identified in 71 (26.9%) of the 264 sides examined in the primary sample, and 61 (22.8%) of the 268 sides examined in the validation sample, respectively.

Results of the side-specific analysis of specimens in the primary sample, as well as data regarding pathologically confirmed capsular invasion and its association with clinical and pathological features, are shown in Table 2. Although MRI findings were judged to be unremarkable in cases that were difficult to evaluate because of residual bleeding or the measurement artifacts, the number of such cases was few (less than 5% of the total). In the analysis of the primary sample, the optimal cut-off values were determined as follows: biopsy Gleason score = 8, serum PSA level = 10.1 ng/mL, number of positive biopsy cores on each side = 2 and maximum percentage of cores positive for cancer on each side = 31%. In the univariate analysis, serum PSA level, biopsy Gleason score ≥8, ≥2 positive biopsy cores on each side, maximum percentage of cores positive for cancer on each side ≥31%, positive DWI MRI findings and positive T2WI MRI findings were significant predictors ($P < 0.05$) of side-specific ECE in the surgical specimens (Table 3). Results for TRUS for each side were almost significant ($P < 0.1$). Multivariate analysis with stepwise selection showed biopsy Gleason scores of ≥8 ($P < 0.005$), DWI MRI-positivity ($P < 0.01$), ≥2 positive biopsy cores on each side ($P < 0.05$) and maximum percentage of cores positive for cancer on each side ≥31% ($P < 0.05$) as significant independent predictors ($P < 0.05$) of side-specific ECE (Table 3). Figure 1 shows representative 3.0-T MRI findings. The predictive accuracy based on each factor is summarized in Table 4. When a combination prediction model was run using any of the four significant predictors (3 biopsy factors in combination with positive DWI MRI findings), 67 of 71 pathologically confirmed ECE sides were correctly predicted in the primary sample (sensitivity 94.4%; 95% CI 86.2–98.4). In addition, four of 66 negatively predicted sides were pathologically determined to have ECE (NPV 93.9%; 95% CI 85.2–98.3%). In the validation sample, the sensitiv-

Table 2 Association of pathologically confirmed prostatic capsular invasion in each lobe with preoperative clinicopathological features in the primary sample

Factors	No. lobes, *n* (%)			
Pathological extent of prostatic capsular invasion	Non-ECE		ECE	Total
	No capsular contact	Capsular contact		
Total no. each lobes	62	131	71	264
Serum PSA value				
Less than 4.0	4 (6.5)	5 (3.8)	1 (1.4)	10 (3.8)
4.1–10.0	39 (62.9)	80 (61.1)	33 (46.5)	152 (57.6)
10.1–20.0	14 (22.6)	31 (23.7)	23 (32.4)	68 (25.8)
≥20.1	5 (8.1)	15 (11.5)	14 (19.7)	34 (12.9)
DRE findings for each side				
Non-palpable	48 (77.4)	93 (71.0)	47 (66.2)	188 (71.2)
Palpable	14 (22.6)	38 (29.0)	24 (33.8)	76 (28.8)
TRUS findings for each side				
Unremarkable	44 (71.0)	85 (64.9)	39 (54.9)	168 (63.6)
Echogenic	18 (29.0)	46 (35.1)	32 (45.1)	96 (36.4)
Biopsy Gleason score/patient				
6 or less	5 (8.1)	11 (8.4)	4 (5.6)	20 (7.6)
3 + 4	23 (37.1)	73 (55.7)	22 (31.0)	118 (44.7)
4 + 3	27 (43.5)	43 (32.8)	28 (39.4)	98 (37.1)
≥8	7 (11.3)	4 (3.1)	17 (23.9)	28 (10.6)
Biopsy results for each side				
No. positive cores				
0	34 (54.8)	20 (15.3)	7 (9.9)	61 (23.1)
1	17 (27.4)	32 (24.4)	9 (12.7)	58 (22.0)
2	7 (11.3)	23 (17.6)	15 (21.1)	45 (17.0)
≥3	4 (6.5)	56 (42.7)	40 (56.3)	100 (37.9)
Maximum percentage of positive cores on each side				
0%	34 (54.8)	20 (15.3)	7 (9.9)	61 (23.1)
1–10%	15 (24.2)	25 (19.1)	10 (14.1)	50 (18.9)
11–30%	11 (17.7)	49 (37.4)	9 (12.7)	69 (26.1)
31–50%	1 (1.6)	11 (8.4)	19 (26.8)	31 (11.8)
51–100%	1 (1.6)	26 (19.8)	26 (36.6)	53 (20.1)
MRI judgments on each side				
T2WI MRI				
Unremarkable	39 (62.9)	38 (29.0)	7 (9.9)	84 (31.8)
Confined cancer without capsular contact	11 (17.7)	19 (14.5)	11 (15.5)	41 (15.5)
Capsular contact	11 (17.7)	52 (39.7)	27 (38.0)	90 (34.1)
ECE (T2WI MRI positive)	1 (1.6)	22 (16.8)	26 (36.6)	49 (18.6)
DWI MRI				
Unremarkable	41 (66.1)	44 (33.6)	14 (19.7)	99 (37.5)
Confined cancer without capsular contact	12 (19.4)	15 (11.5)	6 (8.5)	33 (12.5)
Capsular contact or ECE (DWI MRI-positive)	9 (14.5)	72 (55.0)	51 (71.8)	132 (50.0)

ity, specificity, PPV and NPV of ECE prediction using the proposed model were 93.4% (57/61; 95% CI 84.1–98.2%), 27.5% (57/207; 95% CI 21.6–34.2%), 27.5% (57/207; 95% CI 21.6–34.2%), and 93.4% (57/61; 95% CI 84.1–98.2%), respectively. Therefore, the analysis of the validation sample showed the model to have good reproducibility.

Figure 2 shows a flowchart including all 532 sides categorized using a combination of biopsy information and DWI MRI findings. In total, 94, 111 and 124 of 132 pathologically confirmed ECE cases were correctly predicted using DWI MRI alone, a combination of the three biopsy factors and our prediction model, respectively (sensitivity, 71.2%, 84.1 and 93.9%, respectively). Pathologically confirmed ECE was misdiagnosed by DWI MRI alone in 14.3% patients (38/266), a combination of the three biopsy factors in 11.2% patients (21/188) and our prediction model in

Table 3 Factors predicting pathologically confirmed side-specific extracapsular extension according to univariate and multivariate logistic regression analyses

	Univariate analysis	Multivariate logistic regression analysis	
	P-value	OR (95% CI)	*P*-value
Variables			
Continuous PSA value†	<0.001	1.02 (0.99–1.05)	0.23
≤10.0 ng/mL *vs* ≥10.1 ng/mL	<0.01		
Biopsy Gleason score			
≤7 *vs* ≥8	<0.001	5.66 (2.28–14.0)¶	<0.005
DRE on each side			
Non-palpable *vs* palpable	0.29		
TRUS on each side			
Unremarkable *vs* echogenic	0.08	0.75 (0.38–1.48)	0.41
No. positive biopsy cores on each side			
≤1 *vs* ≥2	<0.001	2.22 (1.05–4.70)¶	<0.05
Maximum percentage of positive cores on each side			
≤30% *vs* ≥31%	<0.001	2.16 (1.07–4.37)¶	<0.05
T2WI MRI			
Negative *vs* positive‡	<0.001	1.78 (0.80–3.94)	0.16
DWI MRI			
Negative *vs* positive§	<0.001	2.39 (1.26–4.54)¶	<0.01

†Wilcoxon rank-sum test with continuity correction. ‡A cancer focus with ECE on T2WI MRI was defined as T2WI MRI positive. §A cancer focus with capsular contact or ECE on DWI MRI was defined as DWI MRI positive. ¶These factors were statistically significant in the final model, and the OR of the final model are shown.

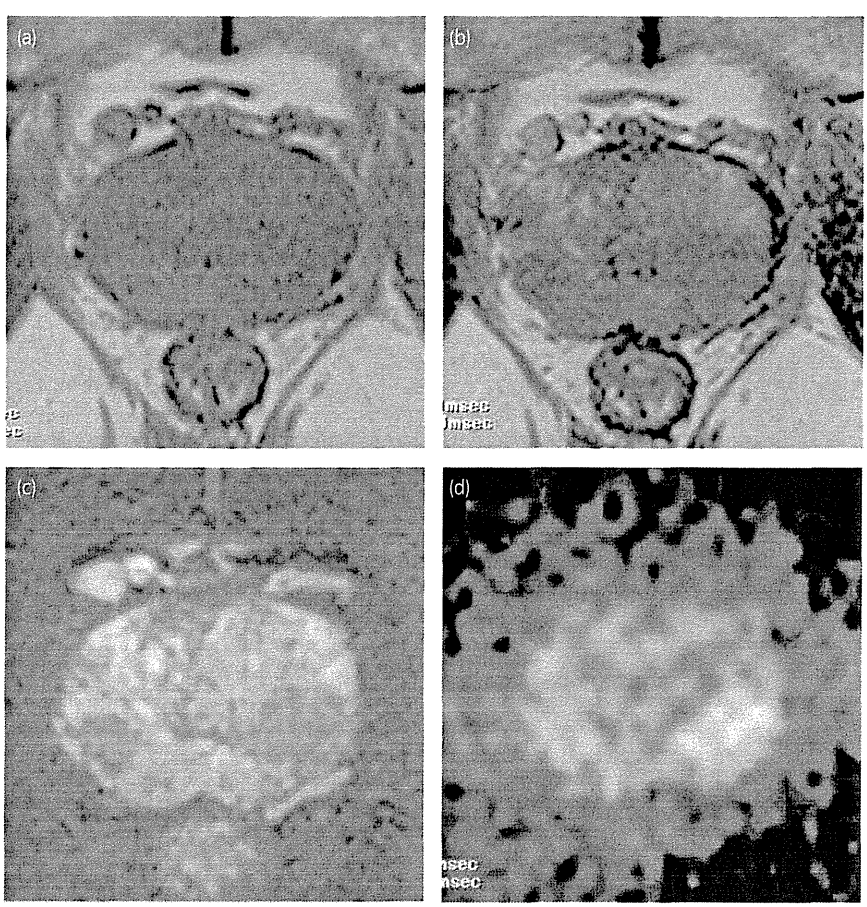

Fig. 1 Representative data of a prostate cancer patient shows the pathological ECE cancer in the peripheral zone of the left lobe and the capsular contact cancer in the peripheral zone of the right lobe. (a) There is no residual intraprostatic bleeding caused by biopsy on T1WI MRI. (b) T2WI MRI and (c) T2WI MRI with fat suppression show the ECE cancer focus in the left lobe and the capsular contact cancer focus in the right lobe. (d) DWI MRI shows a positive cancer focus on both sides.

Table 4 Performance characteristics predicting pathologically confirmed side-specific ECE in the primary sample (264 lobes)

	Sensitivity (%) (95% CI)	Specificity (%) (95% CI)	PPV (%) (95% CI)	NPV (%) (95% CI)	Diagnostic accuracy (%) (95% CI)	Odds ratio
Predictors for pathological ECE cancer						
Biopsy Gleason score ≥8	23.9 (17/71) (14.6–35.5)	94.3 (182/193) (90.0–97.1)	60.7 (17/28) (40.6–78.5)	77.1 (182/236) (71.2–82.3)	75.4 (69.7–80.5)	5.17 (2.14–13.0)
DWI MRI-positive	71.8 (51/71) (59.9–81.9)	58.0 (112/193) (50.7–65.1)	38.6 (51/132) (30.3–47.5)	84.8 (112/132) (77.6–90.5)	61.7 (55.6–67.6)	3.51 (1.89–6.72)
Positive biopsy cores ≥2 on each side	77.5 (55/71) (66.0–86.5)	53.4 (103/193) (46.1–60.6)	37.9 (55/145) (30.0–46.4)	86.6 (103/119) (79.1–92.1)	59.8 (53.7–65.8)	3.91 (2.04–7.86)
Maximum percentage of positive cores ≥31% on each side	52.1 (37/71) (39.9–64.1)	75.6 (146/193) (69.0–81.5)	44.0 (37/84) (33.2–55.3)	81.1 (146/180) (74.6–86.5)	69.3 (63.4–74.8)	3.36 (1.83–6.21)
Combination prediction model†	94.4 (67/71) (86.2.5–98.4)	32.1 (62/193) (25.6–39.2)	33.8 (67/198) (27.3–40.9)	93.9 (62/66) (85.2 × 98.3)	48.9 (42.7–55.1)	7.88 (2.75–31.1)

†In combination with biopsy Gleason score ≥8, DWI MRI positivity, positive biopsy cores ≥2 on either side, or maximum percentage of positive cores ≥31% on either side.

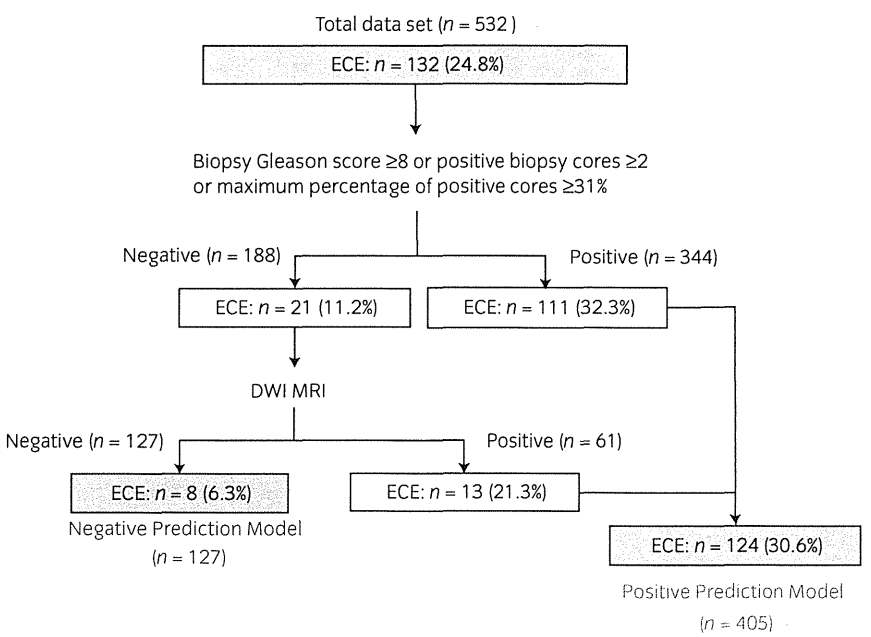

Fig. 2 Flowchart beginning with 532 prostate sides in the total study sample (□). A positive prediction model for ECE is shown (□) through a combination of biopsy information and 3.0-T DWI MRI. A negative prediction model is also shown (□).

6.3% patients (8/127; NPV 85.7%, 88.8% and 93.7%, respectively). OR were 3.27 (95% CI 2.10–5.16), 3.78 (95% CI 2.25–6.62) and 6.55 (95% CI 3.09–16.0) for DWI MRI alone, a combination of the three biopsy factors and our prediction model, respectively. Therefore, sensitivity (93.9% *vs* 84.1%) and NPV (93.7% *vs* 88.8%) were higher for the prediction model than for the combination of the three biopsy factors. Additional DWI MRI information correctly predicted 13 (61.9%) of 21 pathologically confirmed ECE sides that were incorrectly predicted by a combination of the three biopsy factors. However, the specificity (29.8%) and PPV (30.6%) of our prediction model were low.

Discussion

Recent studies have shown improvements in prostate cancer diagnosis with the use of 3.0-T MRI, including DWI.[1] Several studies have also shown the usefulness of T2WI MRI in combination with DWI MRI for improving cancer detection.[3,4,14,15] In one study, cancer detection by T2WI in the TZ

was reportedly inferior to that in the PZ.[13] DWI improved cancer detection rate in the TZ, although DWI sensitivity for cancer in TZ was still lower than that in PZ.[14] Other recently published reports have shown a significant correlation between DWI/ADC values and cancer cell density, Gleason grade, and D'Amico clinical risk scores.[12,14] Well-differentiated cancers of predominant glandular composition yield relatively higher ADC values.[14] In our series, cancer lesions evaluated with 3.0-T DWI MRI imaging were positively associated with high Gleason score, TZ location and higher cancer volume. In contrast, small lesions (<5 mm in diameter) were frequently missed in prostatectomy specimens (data not shown). Therefore, 3.0-T DWI MRI might be useful in predicting the aggressiveness of prostate cancer.

In the current study, the 12-core-biopsy technique and pathological analysis were standard procedures for patients in the primary sample. The results using the model constructed on the basis of data from the primary sample were reproducible in the validation sample. This model predicted side-specific ECE with high sensitivity (93.9%) and NPV (93.7%) compared with conventional biopsy information alone. However, specificity (29.8%) and PPV (30.6%) were low. Our model was useful in the evaluation of non-ECE sides, but just 23.9% patients fit the model. Therefore, the proposed model was reliable only for predicting non-ECE sides. Other limitations included the retrospective nature of the study and sample selection bias. Prostatectomy is carried out at our institution for high-risk and relatively high-risk prostate cancer patients.[13] Therefore, the percentage of patients with clinical stage T3a cancer was higher than that seen at other institutions. In addition, MRI images were evaluated subjectively by two radiologists, and PPV for cancer detection using 3.0-T DWI MRI alone was still low because of the low image resolution.

In conclusion, the present study identified the correlation of conventional preoperative features and 3.0-T DWI MRI with side-specific ECE detection in prostatectomy specimens. 3.0-T DWI MRI evaluation was an independent variable that significantly predicted side-specific ECE. The findings of 3.0-T DWI MRI combined with the evaluation of conventional preoperative features might assist in predicting side-specific non-ECE. Our ECE prediction model that uses the biopsy Gleason score and factors associated with tumor location (DWI MRI positivity, positive biopsy core and maximum percentage of positive cores) has a high NPV, but a low PPV. Nevertheless, it was reproducible in a validation sample; therefore, it might be useful for predicting non-ECE sides.

Acknowledgments

This study was supported by grants from the Ministry of Health and Welfare for the Third-term Comprehensive 10-year Strategy for Cancer Control.

Conflict of interest

None declared.

References

1 Dickinson L, Ahmed HU, Allen C *et al.* Magnetic resonance imaging for the detection, localisation, and characterisation of prostate cancer: recommendations from a European Consensus Meeting. *Eur. Urol.* 2011; **59**: 477–94.
2 Zelhof B, Pickles M, Liney G *et al.* Correlation of diffusion-weighted magnetic resonance data with cellularity in prostate cancer. *BJU Int.* 2009; **103**: 883–8.
3 Nishida S, Kinoshita H, Mishima T, Kurokawa H, Sakaida N, Matsuda T. Prostate cancer detection by prebiopsy 3.0-Tesla magnetic resonance imaging. *Int. J. Urol.* 2011; **18**: 653–8.
4 Jeong IG, Kim JK, Cho KS *et al.* Diffusion-weighted magnetic resonance imaging in patients with unilateral prostate cancer on extended prostate biopsy: predictive accuracy of laterality and implications for hemi-ablative therapy. *J. Urol.* 2010; **184**: 1963–9.
5 Ohori M, Kattan MW, Koh H *et al.* Predicting the presence and side of extracapsular extension: a nomogram for staging prostate cancer. *J. Urol.* 2004; **171**: 1844–9.
6 Kupelian PA, Katcher J, Levin HS, Klein EA. State T1-2 prostate cancer: a multivariate analysis of factors affecting biochemical and clinical failures after radical prostatectomy. *Int. J. Radiat. Oncol. Biol. Phys.* 1997; **37**: 1043–52.
7 Graefen M, Walz J, Huland H. Open retropubic nerve-sparing radical prostatectomy. *Eur. Urol.* 2006; **49**: 38–48.
8 Gontero P, Kirby RS. Nerve-sparing radical retropubic prostatectomy: techniques and clinical considerations. *Prostate Cancer Prostatic Dis.* 2005; **8**: 133–9.
9 Wheeler TM, Dillioglugil O, Kattan MW *et al.* Clinical and pathological significance of the level and extent of capsular invasion in clinical stage T1-2 prostate cancer. *Hum. Pathol.* 1998; **29**: 856–62.
10 Sobin LH, Gospodarowicz MK, Wittekind CH (eds) *TNM Classification of Malignant Tumors UICC International Union Against Cancer*, 7th edn. Wiley-Blackwell, New York, 2009; 243–8.
11 Bloch BN, Furman-Haran E, Helbich TH *et al.* Prostate cancer: accurate determination of extracapsular extension with high-spatial-resolution dynamic contrast-enhanced and T2-weighted MR imaging – initial results1. *Radiology* 2007; **245**: 176–85.
12 Team RDC. *R: A Language and Environment for Statistical Computing*. R Foundation for Statistical Computing, Vienna, Austria, 2011.
13 Miyake H, Fujimoto H, Komiyama M, Fujisawa M. Development of "extended radical retropubic prostatectomy": a surgical technique for improving margin positive rates in prostate cancer. *Eur. J. Surg. Oncol.* 2010; **36**: 281–6.
14 Tan C, Wang J, Kundra V. Diffusion weighted imaging in prostate cancer. *Eur. Radiol.* 2011; **21**: 593–603.
15 Haider MA, van der Kwast TH, Tanguay J *et al.* Combined T2-weighted and diffusion-weighted MRI for localization of prostate cancer. *AJR Am. J. Roentgenol.* 2007; **189**: 323–8.

JJCO Japanese Journal of Clinical Oncology

Jpn J Clin Oncol 2012;42(11)1066–1072
doi:10.1093/jjco/hys136
Advance Access Publication 22 August 2012

Characteristics of Lymph Node Metastases Defining the Outcome After Radical Cystectomy of Urothelial Bladder Carcinoma

Tohru Nakagawa[1,*], Yae Kanai[2], Hiroyuki Nakanishi[1], Motokiyo Komiyama[1] and Hiroyuki Fujimoto[1]

[1]Department of Urology, National Cancer Center Hospital and [2]Division of Molecular Pathology, National Cancer Center Research Institute, Tokyo, Japan

*For reprints and all correspondence: Tohru Nakagawa, Department of Urology, National Cancer Center Hospital, 5-1-1 Tsukiji, Chuo-ku, Tokyo 104-0045, Japan. E-mail: tohru-tky@umin.ac.jp

Received June 10, 2012; accepted July 29, 2012

Objective: The aim of this study was to identify clinicopathological variables associated with the clinical outcomes of patients with lymph node metastasis-positive urothelial bladder carcinoma after radical cystectomy.
Methods: Forty-six patients who underwent radical cystectomy without preoperative chemotherapy and had histologically proven nodal metastasis were included in the study. The status of lymph nodes and primary lesion was analyzed in terms of disease-specific survival and recurrence-free survival.
Results: The 5-year disease-specific survival and recurrence-free survival for the 46 patients overall were 41.3 and 32.2%, respectively. Univariate analysis showed that pN status, the total number of involved lymph nodes, lymph node density and extranodal invasion were statistically significant variables predictive of disease-specific survival. Multivariate analysis revealed that the total number of involved lymph nodes, extranodal invasion and diameter of the metastatic lesion were statistically significant variables predictive of disease-specific survival. Interestingly, the diameter of metastatic lesions was inversely correlated with poorer survival. Patients with large ($\geq$10 mm) metastatic lesions and no extranodal invasion (expansive growth) had significantly better disease-specific survival than those with multiple small ($<$10 mm) metastatic lesions and no extranodal invasion (highly spreading) ($P = 0.0156$) or those with extranodal invasion (infiltrative growth) ($P = 0.0181$).
Conclusions: Our data indicate that the clinical outcome of node-positive patients is not only stratified according to the tumor burden reflected in the total number of involved lymph nodes, but also affected by tumor biology including invasiveness and potential for metastasis, which is reflected in pathological characteristics such as extranodal invasion and the diameter of metastatic lesions.

Key words: bladder cancer – extranodal invasion – lymph node – metastasis – radical cystectomy

INTRODUCTION

Radical cystectomy with pelvic lymph node (LN) dissection is a gold standard treatment for muscle-invasive bladder cancer (1); 18–28% of the patients who undergo radical cystectomy are found to have LN metastases upon histological examination of their surgically resected specimens (1). The 5-year overall survival and recurrence-free survival (RFS) of patients with LN metastases (pN1–3) are reported to be 25–31 and 20–35%, respectively (2), and their clinical outcomes are highly variable.

Several clinicopathological factors that can further stratify the risk of recurrence and death in node-positive patients have been identified: the number of LNs involved with the tumor (3–7), the number of LNs removed (5,7), the ratio (percentage) of the number of involved nodes divided by the total number of nodes removed (LN density) (4,5,8–11), primary pathological stage (pT) (3–5), extranodal invasion

(ENI) of LN metastases (12–14) and the use of adjuvant chemotherapy (6,15).

Among these variables, the significance of the total number of LNs involved with the tumor and LN density have been well examined and are becoming accepted as prognostic variables, although the use of LN density in a practical setting is still debatable (16).

On the other hand, the significance of the diameter of metastatic lesions in LNs and ENI for survival prediction remains to be clarified. Although Mills et al. (12) reported that metastatic lesions in LNs <0.5 cm in diameter were associated with better clinical outcome, no subsequent studies have validated such an association. Moreover, the conclusions of previous studies that examined the significance of ENI for predicting the survival of patients with bladder cancer were inconsistent. Although three papers from a single center (the University of Bern, Switzerland) have suggested that ENI is the strongest independent prognostic factor for disease-specific survival (DSS) (12–14), Kassouf et al. (15) reported that ENI was associated with neither DSS nor RFS.

The aim of this study was to assess the significance of several clinicopathological variables including ENI and the diameter of metastatic lesions for the prediction of outcome in patients with LN metastasis-positive urothelial carcinoma of the urinary bladder after cystectomy.

PATIENTS AND METHODS

We retrospectively reviewed the medical records of 611 consecutive patients who underwent radical cystectomy and pelvic LN dissection for invasive bladder cancer with curative intent at the National Cancer Center Hospital between January 1986 and April 2008. During this period, radical cystectomy was abandoned in 25 patients intraoperatively due to advanced local disease. Patients included in the study were those for whom LN metastases were confirmed histologically in their surgically resected specimens. Patients were excluded if they had received neoadjuvant chemotherapy before surgery, had pure non-urothelial carcinomas histologically (i.e. squamous cell carcinoma and adenocarcinoma), had remote metastases at the time of surgery or had synchronous or metachronous invasive upper urinary tract cancers. On this basis, 46 patients were included in the present study, which comprised 7.5% of the 611 patients who underwent radical cystectomy. This study was approved for analysis by the institutional review board.

All cystectomy specimens were subjected to routine pathological examination. The LN specimen from each anatomical location was separately examined visually and by manual palpation without fat clearing solution, and all macroscopically detected LNs were completely embedded. One hematoxylin- and eosin-stained section was taken per tissue block, and no immunostains were routinely performed. A single pathologist (Y.K.) reviewed the specimens microscopically for this study in a blinded manner. The primary tumors and LNs were staged based on the 2009 UICC TNM system (17) and were evaluated for the diameter of metastatic lesions in the LNs, and the presence or absence of ENI. ENI was defined as obvious disruption of the microscopically visible LN capsule by tumor cells infiltrating into the perinodal tissue (Fig. 1).

All patients were followed routinely after surgery every 3 months in the first year, at 3- to 6-month intervals in years 2–3, every 6 months in years 4–5 and annually thereafter. Follow-up consisted of physical examination, serum biochemical profile, urine cytology, chest X-ray or computed tomography (CT) imaging of the chest and CT imaging of the abdomen–pelvis.

Survival data were analyzed using the Kaplan–Meier method, and log-rank tests were used to evaluate associations between survival and the variables studied. The duration of follow-up was calculated from the date of surgery to the date of death or last follow-up. Univariate and multivariate Cox

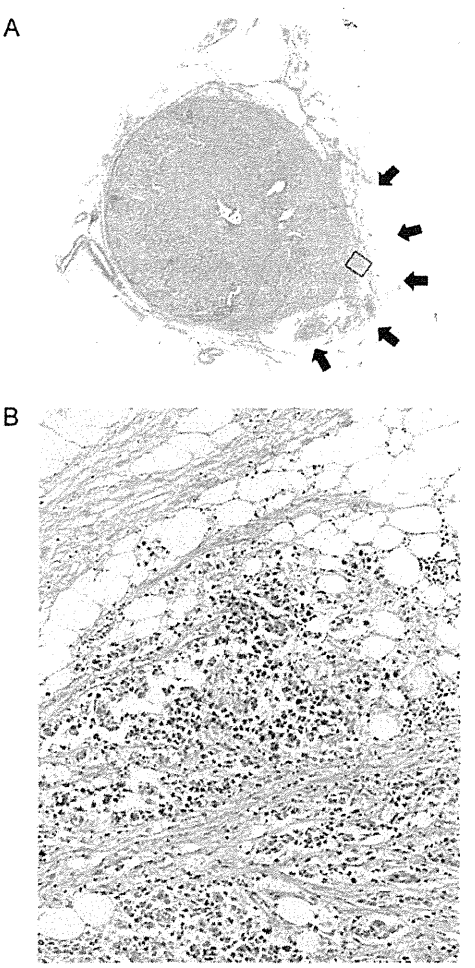

Figure 1. A representative photograph of lymph node (LN) metastasis with extranodal invasion. LN capsule is disrupted by tumor cells infiltrating into the perinodal tissue (arrows). (A) Scanning magnification. (B) Higher magnification of the boxed area in (A) (reduced from ×200).

proportional hazard models were employed to assess which clinicopathological features were associated with death due to, or recurrence of, bladder cancers. The relationships between the clinicopathological features studied and outcome were summarized in terms of risk ratios and 95% confidence intervals (95% CI). Differences with P values of <0.05 were considered significant.

RESULTS

The clinicopathological features of the 46 patients included in the study are shown in Table 1. There were 37 male and 9 female patients, with a median age of 66 (range: 46–83) years at the time of surgery. The median follow-up duration was 32 (range: 3–272) months for the patients as a whole and 110.5 (range: 26–272) months for the 14 patients who were alive at the final follow-up.

Thirty-three patients suffered from disease recurrence, and 28 of them died of metastatic bladder cancer during follow-up. The 5-year DSS and RFS for the 46 patients overall were 41.3 and 32.2%, respectively (Fig. 2). The median DSS and RFS were 34 (95% CI: 25–154) and 11.5 (95% CI: 10–46) months, respectively (Fig. 2).

Due to the retrospective nature of this study, the extent of LN dissection was variable; 36 patients underwent limited pelvic lymphadenectomy below the bifurcation of common iliac arteries, whereas 7 and 3 cases up to the level of aortic bifurcation and inferior mesenteric artery, respectively.

Adjuvant systemic chemotherapy was considered for all cases with LN metastasis. However, it was not administered in 28 patients because of impaired performance status and/or high age, or no consent from the patients. The regimens of chemotherapy were two courses of MVAC (methotrexate, vinblastine, doxorubicin and cisplatin) in 16 cases, MEP (methotrexate, etoposide and cisplatin) in 1 and CAP (cyclophosphamide, doxorubicin and cisplatin) in 1.

The results of univariate analysis to examine the contribution of each clinicopathological factor to DSS and RFS are shown in Table 2. Whereas pT3–4 tumors did not show significant difference compared with pT2 tumors in terms of DSS and RFS, several LN-related variables were found to be significantly associated with patient prognosis. Therefore, further analyses focused on these LN-related variables. pN status according to the TNM classification, the total number of involved LNs, LN density and ENI were statistically significant variables predictive of DSS, and the total number of involved LNs and LN density were significant variables predictive of RFS. Figure 3 shows DSS of the patients with or without ENI and of the patients with less than five involved LNs or with five or more, analyzed using the Kaplan–Meier method.

Multivariate analysis revealed that the total number of involved LNs, ENI and the diameter of the metastatic lesion

Table 1. Clinicopathological characteristics of the 46 patients with lymph node metastasis at radical cystectomy

Sex	
Male	37 (80.4%)
Female	9 (19.6%)
Age	
Median	66
Range	46–83
Extent of LN dissection	
Below bifurcation of CIA	36 (78.3%)
Up to aortic bifurcation	7 (15.2%)
Up to the level of IMA	3 (6.5%)
Histological type	
UC	38 (82.6%)
UC with other components (i.e. squamous cell carcinoma and adenocarcinoma)	8 (17.4%)
Nuclear grade	
G3	46 (100%)
pT stage	
pT2	6 (13.0%)
pT3	26 (56.5%)
pT4	14 (30.5%)
pN stage	
pN1	16 (34.8%)
pN2	25 (54.3%)
pN3	5 (10.9%)
Total number of involved LNs	
Median	2
Range	1–13
Number of LNs resected	
Median	12.5
Range	4–36
LN density	
Median	17%
Range	3–67
Maximum diameter of metastatic lesions in LNs	
Median	9 mm
Range	1–28
ENI of LN metastases	
Negative	27 (58.7%)
Positive	19 (41.3%)
Adjuvant chemotherapy	
No	28 (60.9%)
Yes	18 (39.1%)

LN, lymph node; CIA, common iliac artery; IMA, inferior mesenteric artery; UC, urothelial carcinoma; ENI, extranodal invasion.

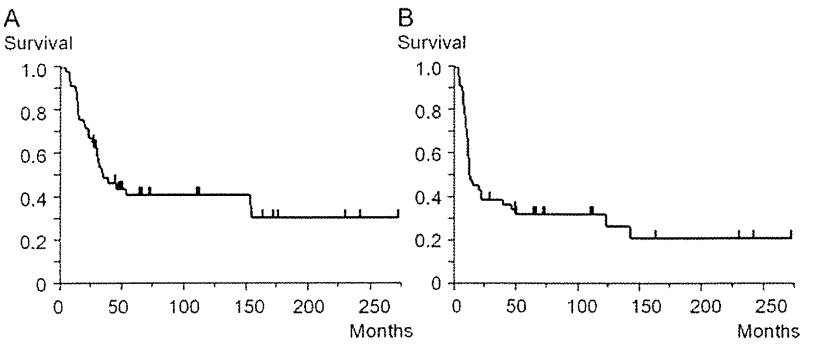

Figure 2. Disease-specific (A) and recurrence-free (B) survival for the patients overall analyzed by the Kaplan–Meier method.

Table 2. Univariate analyses of variables predicting disease-specific and recurrence-free survival

	P value	
	DSS	RFS
Extent of LN dissection		
Below vs. above iliac bifurcation	0.2042	0.1590
Histological type		
Mixed vs. pure UC	0.6140	0.7633
pT		
pT3–4 vs. pT2	0.1097	0.2830
pN		
pN2–3 vs. pN1	0.0224	0.0732
Total number of involved LNs (continuous)	0.0008	0.0018
Number of nodes resected (continuous)	0.9555	0.6407
LN density (continuous)	0.0112	0.0128
Maximum diameter of metastatic lesion in LN (continuous)	0.8079	0.8015
ENI of LN metastases		
Positive vs. negative	0.0338	0.0767
Adjuvant chemotherapy		
Yes vs. no	0.5230	0.0828

DSS, disease-specific survival; RFS, recurrence-free survival; UC, urothelial carcinoma.

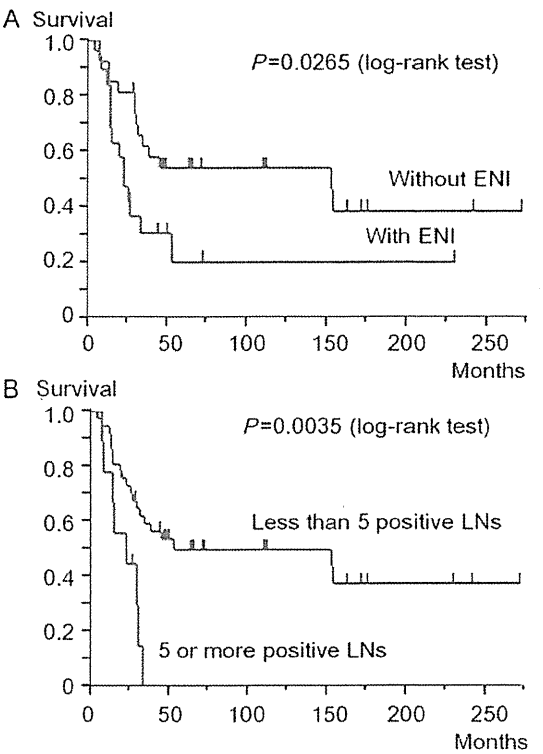

Figure 3. Disease-specific survival of patients with and without extranodal invasion (ENI) (A) and that of patients with fewer than five involved LNs or with 5 or more (B), analyzed by the Kaplan–Meier method.

were statistically significant variables predictive of DSS (Table 3). For RFS, the total number of involved LNs was the only variable showing a statistically significant correlation (Table 3).

Thus, ENI, the total number of positive nodes and the diameter of metastatic lesions were independently associated with DSS. Interestingly, the diameter of metastatic lesions was inversely correlated with poorer survival: some patients had a good outcome despite having sizable metastatic nodes. In fact, those with ENI-negative, large (>10 mm) metastatic nodes (seven patients) showed favorable clinical outcome. They showed better DSS and RFS than those with ENI-negative, multiple small metastatic lesions (<10 mm) (eight patients) ($P = 0.0156$ for DSS and $P = 0.0483$ for RFS). They also showed better DSS and marginally better RFS than those with ENI-positive nodes (19 patients) ($P = 0.0181$ for DSS and $P = 0.0527$ for RFS) (Figs 4 and 5).

DISCUSSION

The presence of histologically proven LN metastases is an adverse prognostic factor in patients who undergo radical cystectomy for bladder cancer with curative intent. However,

Table 3. Multivariate analyses of variables predicting disease-specific and recurrence-free survival

	Disease-specific survival		Recurrence-free survival	
	Risk ratio (95% CI)	*P* value	Risk ratio (95% CI)	*P*-value
Total number of involved LNs (continuous)	1.51 (1.21–1.89)	0.0003	1.31 (1.11–1.52)	0.0018
Maximum diameter of metastatic lesion in LN (continuous, unit: mm)	0.91 (0.84–0.99)	0.0214		
ENI				
Positive vs. negative	2.50 (1.02–6.09)	0.0445		

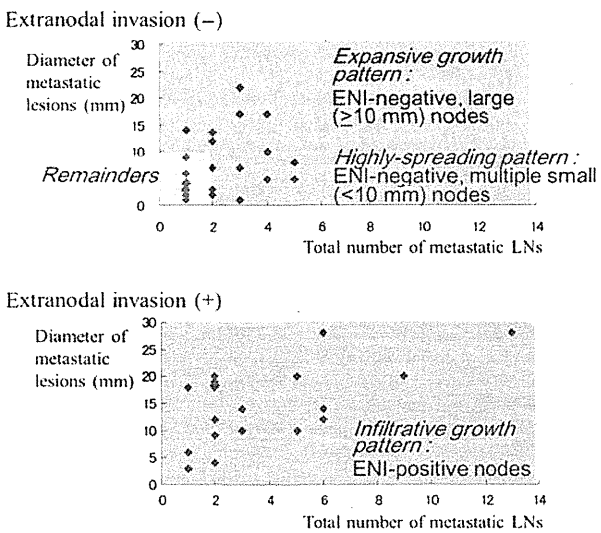

Figure 4. Distribution of the diameter of metastatic lesions and the number of involved LNs in the 27 patients with LN metastases without ENI and in the 19 patients with ENI.

the clinical outcome of patients with LN metastases is variable, and several clinicopathological factors have been reported to further stratify the risk of recurrence and death in such patients.

In our present study, the number of metastasis-positive nodes was the most significant variable predictive of poor survival. Patients with five or more positive nodes had a significantly worse outcome than those with fewer than five positive nodes ($P = 0.0035$ for DSS and $P = 0.0006$ for RFS). Previous studies have also reported similar data using cut-off points of 5, 6 and 8 for the number of LNs in order to discriminate groups with good or poor prognosis (3–6).

ENI is reported to represent an aggressive feature of metastatic cancers and to be a significant predictor of poorer outcome in cancers of the kidney, breast, lung, colon, head and neck, penis and ampulla of Vater (18–24). Reports examining the significance of ENI in bladder cancer are limited, and their results have been inconsistent. Three papers from a single center (the University of Bern, Switzerland) have suggested that ENI is the strongest independent prognostic factor for DSS (12–14). Two other studies reported that ENI was a significant prognostic factor for DSS in univariate analysis, but did not retain its significance in multivariate analysis (6,25). A paper from the M.D. Anderson Cancer Center reported that ENI was not associated with DSS ($P = 0.43$) or RFS ($P = 0.82$) (15). Thus, the conclusions have been inconsistent, and the prognostic significance of ENI in bladder cancers is still not fully understood. In the present study, ENI was detected in 19 (41.3%) of 46 node-positive patients, consistent with the reported incidence of ENI of 33–68% (6,12–15), and was associated with poorer prognosis of node-positive patients in both univariate and multivariate analyses.

It was somehow surprising that the diameter of metastatic lesions was inversely associated with poorer DSS. We did experience several patients with sizable nodal metastases who were cured with surgery alone or showed an indolent clinical course after tumor recurrence. LN diameter was significantly larger in ENI-positive cases than in ENI-negative ($P = 0.0002$, Mann–Whitney's test), and we focused attention on the outliers of this association; seven cases with ENI-negative, large (>10 mm) metastatic nodes. In fact, these seven cases showed favorable DSS, irrespective of the number of metastasis-positive nodes (Fig. 5). This type of tumors may have limited invasive potential and do not extend beyond the nodal capsule, thus being ENI-negative. In addition, they may have low metastasis potential, and consequently show local proliferation, resulting in a larger metastasis diameter (expansive growth pattern, Fig. 4). In contrast, patients with ENI-positive nodes (19 patients) had dismal clinical outcome (Fig. 5). ENI-positive nodes may represent aggressive invasive potential, resulting in the destruction of the LN capsule and invasion into surrounding tissues (infiltrative growth pattern, Fig. 4). There was a significant ($P < 0.0001$) positive correlation between diameter and total number of positive nodes with a Spearman correlation coefficient of 0.5617. Again, we focused attention on the outliers of this association. As shown in the upper panel of Fig. 4, eight cases had multiple small (<10 mm) LN metastases without ENI. These eight cases also showed poor outcome (Fig. 5). Multiple small LNs may represent spreading ability of cancer cells via lymphatic vessels before they form large metastatic lesions in LNs (highly spreading pattern, Fig. 4). Remainders (single small LN metastasis

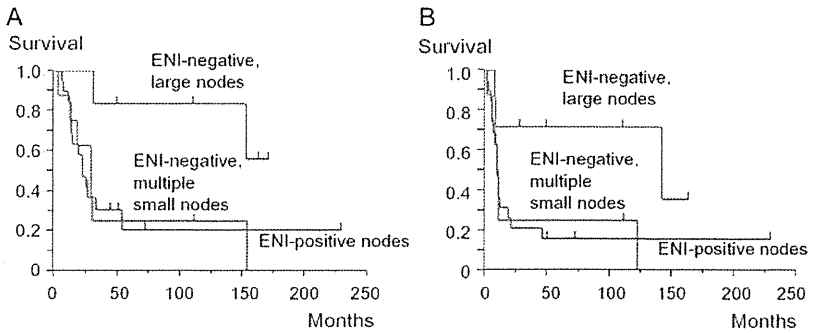

Figure 5. Disease-specific (A) and recurrence-free (B) survival stratified according to LN metastasis patterns, analyzed by the Kaplan–Meier method.

without ENI) were in the early phase of either of the three categories (12 patients).

Our data show that the clinical outcome of node-positive patients is not simply stratified according to well-accepted variables, such as the number of positive nodes, that reflect the tumor burden. It is also affected by tumor biology including properties such as invasiveness and metastasis potential, which is reflected in pathological characteristics such as ENI and the diameter of nodal lesions.

In conclusion, the present study has shown that the total number of involved nodes, ENI and the diameter of metastatic lesions are significantly associated with DSS of patients with node-positive urothelial bladder carcinoma. Differences in the characteristics of metastatic nodes such as expansive growth/infiltrative growth/highly spreading pattern would result in the variable clinical outcome. Even the patients with large LN metastases may benefit from meticulous LN dissection if the tumor showed expansive growth pattern.

Acknowledgement

The authors thank Dr Tadao Kakizoe for his supervision of this work.

Conflict of interest statement

None declared.

References

1. Stein JP, Skinner DG. Radical cystectomy for invasive bladder cancer: long-term results of a standard procedure. *World J Urol* 2006;24:296–304.
2. Karl A, Carroll PR, Gschwend JE, et al. The impact of lymphadenectomy and lymph node metastasis on the outcomes of radical cystectomy for bladder cancer. *Eur Urol* 2009;55:826–35.
3. Lerner SP, Skinner DG, Lieskovsky G, et al. The rationale for en bloc pelvic lymph node dissection for bladder cancer patients with nodal metastases: long-term results. *J Urol* 1993;149:758–64.
4. Stein JP, Lieskovsky G, Cote R, et al. Radical cystectomy in the treatment of invasive bladder cancer: long-term results in 1,054 patients. *J Clin Oncol* 2001;19:666–75.
5. Stein JP, Cai J, Groshen S, Skinner DG. Risk factors for patients with pelvic lymph node metastases following radical cystectomy with en bloc pelvic lymphadenectomy: concept of lymph node density. *J Urol* 2003;170:35–41.
6. Frank I, Cheville JC, Blute ML, et al. Transitional cell carcinoma of the urinary bladder with regional lymph node involvement treated by cystectomy: clinicopathologic features associated with outcome. *Cancer* 2003;97:2425–31.
7. Wright JL, Lin DW, Porter MP. The association between extent of lymphadenectomy and survival among patients with lymph node metastases undergoing radical cystectomy. *Cancer* 2008;112:2401–8.
8. Herr HW. Superiority of ratio based lymph node staging for bladder cancer. *J Urol* 2003;169:943–5.
9. Kassouf W, Leibovici D, Munsell MF, Dinney CP, Grossman HB, Kamat AM. Evaluation of the relevance of lymph node density in a contemporary series of patients undergoing radical cystectomy. *J Urol* 2006;176:53–7.
10. Kassouf W, Agarwal PK, Herr HW, et al. Lymph node density is superior to TNM nodal status in predicting disease-specific survival after radical cystectomy for bladder cancer: analysis of pooled data from MDACC and MSKCC. *J Clin Oncol* 2008;26:121–6.
11. Osawa T, Abe T, Shinohara N, et al. Role of lymph node density in predicting survival of patients with lymph node metastases after radical cystectomy: a multi-institutional study. *Int J Urol* 2009;16:274–8.
12. Mills RD, Turner WH, Fleischmann A, Markwalder R, Thalmann GN, Studer UE. Pelvic lymph node metastases from bladder cancer: outcome in 83 patients after radical cystectomy and pelvic lymphadenectomy. *J Urol* 2001;166:19–23.
13. Fleischmann A, Thalmann GN, Markwalder R, Studer UE. Extracapsular extension of pelvic lymph node metastases from urothelial carcinoma of the bladder is an independent prognostic factor. *J Clin Oncol* 2005;23:2358–65.
14. Fleischmann A, Thalmann GN, Markwalder R, Studer UE. Prognostic implications of extracapsular extension of pelvic lymph node metastases in urothelial carcinoma of the bladder. *Am J Surg Pathol* 2005;29:89–95.
15. Kassouf W, Leibovici D, Luongo T, et al. Relevance of extracapsular extension of pelvic lymph node metastasis in patients with bladder cancer treated in the contemporary era. *Cancer* 2006;107:1491–5.
16. Herr HW. The concept of lymph node density—is it ready for clinical practice? *J Urol* 2007;177:1273–5.
17. Sobin LH, Gospodarowicz MK, Wittekind CH, editors, International Union Against Cancer (UICC). *TNM Classification of Malignant Tumors*. 7th ed. Hoboken, NJ: Wiley-Blackwell 2009.
18. Dimashkieh HH, Lohse CM, Blute ML, Kwon ED, Leibovich BC, Cheville JC. Extranodal extension in regional lymph nodes is associated with outcome in patients with renal cell carcinoma. *J Urol* 2006;176:1978–82.
19. Altinyollar H, Berberoğlu U, Gülben K, Irkin F. The correlation of extranodal invasion with other prognostic parameters in lymph node positive breast cancer. *J Surg Oncol* 2007;95:567–71.
20. Lee YC, Wu CT, Kuo SW, Tseng YT, Chang YL. Significance of extranodal extension of regional lymph nodes in surgically resected non-small cell lung cancer. *Chest* 2007;131:993–9.

21. Komuta K, Okudaira S, Haraguchi M, Furui J, Kanematsu T. Identification of extracapsular invasion of the metastatic lymph nodes as a useful prognostic sign in patients with resectable colorectal cancer. *Dis Colon Rectum* 2001;44:1838–44.
22. de Carvalho MB. Quantitative analysis of the extent of extracapsular invasion and its prognostic significance: a prospective study of 170 cases of carcinoma of the larynx and hypopharynx. *Head Neck* 1998;20:16–21.
23. Pandey D, Mahajan V, Kannan RR. Prognostic factors in node-positive carcinoma of the penis. *J Surg Oncol* 2006;93:133–8.
24. van der Gaag NA, ten Kate FJ, Lagarde SM, Busch OR, van Gulik TM, Gouma DJ. Prognostic significance of extracapsular lymph node involvement in patients with adenocarcinoma of the ampulla of Vater. *Br J Surg* 2008;95:735–43.
25. Jeong IG, Ro JY, Kim SC, et al. Extranodal extension in node-positive bladder cancer: the continuing controversy. *BJU Int* 2011;108:38–43.

INTERNATIONAL JOURNAL OF
UROLOGY

International Journal of Urology (2011) 18, 876–881 doi: 10.1111/j.1442-2042.2011.02895.x

JUA Cancer Registration Statistics

Oncological outcomes of the prostate cancer patients registered in 2004: Report from the Cancer Registration Committee of the JUA

Hiroyuki Fujimoto,[1,2] Hiroyuki Nakanishi,[1,2] Tsuneharu Miki,[1,3] Yoshinobu Kubota,[1,4] Satoru Takahashi,[1,5] Kazuhiro Suzuki,[1,6] Hiro-omi Kanayama,[1,7] Kazuya Mikami[1,3] and Yukio Homma[1,8]

[1]The Cancer Registration Committee of the Japanese Urological Association, [2]Urology Division, National Cancer Center Hospital, [5]Department of Urology, Nihon University, [8]Department of Urology, Graduate School of Medicine, The University of Tokyo, Tokyo, [3]Department of Urology, Graduate School of Medical Sciences, Kyoto Prefectural University of Medicine, Kyoto, [4]Department of Urology, Yokohama City University Graduate School of Medicine, Yokohama, [6]Department of Urology, Gunma University School of Medicine, Gunma, [7]Department of Urology, School of Medicine, The University of Tokushima, Tokushima, Japan

Objectives: In 2001, the Cancer Registration Committee of the Japanese Urological Association initiated a data collection of prostate cancer patients into a computer-based database. The aim of the present study is to report the clinical and pathological characteristics and outcomes of prostate cancer patients diagnosed in 2004 in Japan.

Methods: Overall, 11 385 patients from 239 institutions were registered into the database. After excluding 1105 patients because of insufficient data, duplication or insufficient follow up, 10 280 patients were eligible for the analysis. Most of them (10 198, 99.2%) were Japanese and 1195 (11.6%) had metastatic disease at the time of diagnosis. The mean and median follow up was 53.2 months and 61.5 months, respectively.

Results: The 5-year overall and prostate cancer-specific survival rate was 89.7% and 94.8%, respectively. The 5-year prostate cancer-specific survival rate of M0 and M1 disease was 98.4% and 61.1%, respectively. For 8424 cases of organ-confined or regional disease, Japanese urologists used as the initial treatment hormone ablation therapy alone (3360, 39.9%), radical prostatectomy (3140, 38.1%), radiation therapy (1530, 18.2%) and watchful waiting (394, 4.7%) including active surveillance or palliative observation.

Conclusions: This is the first large population report of survival data in Japanese prostate cancer patients. In Japan, the disease population, survival period with metastatic disease and ratio of patients having hormone ablation therapy differ from those in Western countries.

Key words: epidemiology, Japanese, prostate neoplasm, registration, survival.

Introduction

In the 1990s, prostate-specific antigen (PSA) testing became widespread in Japan, as in the USA and Europe. The incidence of prostate cancer in Japan also appears to be rising. There is no doubt that PSA screening contributes to earlier diagnosis of prostate cancer. Whether earlier detection of the prostate cancer in Japanese men helps reduce prostate cancer-specific mortality is unknown as a result of the lack of detailed information about Japanese prostate cancer patients.

In 2001, the Japanese Urological Association (JUA) initiated a study to estimate the etiology, diagnosis, initial treatment, pathological findings and final outcomes of prostate cancer using computer-based registration of prostate cancer patients from institutions all over Japan. In 2005, we published the initial report on the registered 4529 prostate cancer patients diagnosed in 2000[1] and the estimated etiology, diagnosis and initial planned treatment were analyzed. In 2010, detailed information including the main treatment modality used, adjuvant therapies used and survival of prostate cancer patients diagnosed in 2004 was collected to assess the current situation of prostate cancer in Japan.

Correspondence: Hiroyuki Fujimoto M.D., Urology Division, National Cancer Center Hospital, 5-1-1 Tsukiji, Chuo-ku, Tokyo 104-0045 Japan. Email: juacr@nifty.com; hfujimot@ncc.go.jp

Received 30 August 2011; accepted 4 October 2011.

Methods

Patients and treatments

In 2010, data on patients diagnosed with prostate cancer in 2004 were collected, along with 5-year survival data and radical prostatectomy pathology results. Incidental cancer found within specimens removed during radical cystoprostatectomy for bladder cancer and transitional cell carcinoma of the prostate concomitant with bladder cancer were excluded from this registry. In all, 11 385 patients were

registered from 239 institutions. Excluded from the analysis were 37 duplications (only one record was removed and the patient remained in the registry), six patients because of insufficient data and 1062 patients with less than 180 days of follow up, leaving 10 280 patients included in the analysis.

Variables

Pathological staging was based on the fifth edition of the TNM classification and the third edition of the General Rule for Clinical and Pathological Studies on Prostate Cancer (2001).[2] For the PSA analysis, only cases measured with the Tandem-R kit PSA assay ($n = 4567$, 44.4%) were included to avoid statistical scatter. The definition of PSA failure was determined based on the clinician's judgement.

Survival data were analyzed according to the main treatment modality and the M stage. The initial main treatment modalities used were categorized into four groups: hormone ablation therapy alone (Hx), radical prostatectomy (RP) with or without neoadjuvant hormone treatment (NHT), radiation therapy (Rx) with or without NHT and watchful waiting (W/W) including active surveillance or palliative observation irrespective of the intent. Characteristics and outcomes from the four treatment groups were analyzed separately.

Analysis of progression-free survival was not possible as a result of difficulties in timing recurrence correctly. In some RP cases, adjuvant therapy was initiated just after the operation on the basis of the pathological findings. In addition, there were substantial differences in how post-Rx PSA failure was defined. For these reasons, the exact timing of recurrence was not able to be determined for a sizable number of patients, whom we consequently described as having "stable disease." Therefore, we had no other choice but to focus on the mortality rate, overall survival (OS) and prostate cancer-specific survival (PCSS).

Statistical methods

For statistical analysis, Student's *t*-test was used for analysis of intergroup differences in means and the χ^2-test was used for intergroup comparisons. Survival data was analyzed by the Kaplan–Meier method.

Results

Overall data

The registered patients' characteristics including age, PSA, Gleason score and TNM classification were summarized according to the main initial treatment modality (see Table S1, supporting information). In the 10 280 patients, the number of the patients treated by Hx, RP, Rx and W/W was 4934 (49.8%), 3212 (31.5%), 1605 (10.4%) and 485 (4.7%), respectively. The 44 patients were treated by other modalities. There were statistically significant differences among patients in different treatment groups. Patients treated with RP were the youngest (median age 68.0 years), with patients treated with Hx on average approximately 8.5 years older (median age 76.0 years). Overall, median PSA at diagnosis was 13.0 ng/mL, but the median PSA within the W/W group was 7.3 ng/mL, which was the lowest. Median Gleason score was 7 among Hx, RP and Rx groups, and 6 in W/W patients. Approximately 50–60% of each group was staged as T1c or T2 disease. In contrast, 11.5% of patients presented with metastatic disease at the time of diagnosis.

The 5-year OS and PCSS of all 10 280 patients was 98.7% and 94.8%, respectively. Figure 1 shows the Kaplan–Meier curves according to M stage. Bony disease (M1b) comprised the majority of M1 patients. The 5-year OS and PCSS was 61.8% and 66.7%, respectively. In M1 disease, there was a significant correlation between survival and Gleason score ($P < 0.001$).

T1-4N0M0 prostate cancer

There were 8424 patients with T1-4N0M0 prostate cancer. The distribution and proportion of clinical T (cT) stage and age by treatment group are shown in Figure 2. Interestingly, in Japan more than 30% of patients received Hx as the main treatment modality across all cT stages. Even for cT1 or cT2 disease, RP, Hx and Rx were carried out in approximately 50%, 30% and 20% of the cases, respectively. The age distribution differed dramatically across treatment groups. For patients less than 75 years-of-age, RP was widely used. Rx was carried out at similar rates (approximately 20%) in patients up to 80 years-of-age. Hx was the major treatment in patients over 80 years-of-age.

OS and PCSS in T1-4N0M0 disease by treatment group were shown to be 97.6% and 99.6% in RP, 95.6% and 98.5% in Rx, 96.4% and 99.7% in W/W and 88.9% and 97.7% in Hx. Five-year PCSS for patients without metastatic disease was excellent (98.4%).

Distribution of age and PSA in patients with T1-4N0M0 prostate cancer according to treatment was shown in Figure S1. Figure S2 shows cT distribution and the main treatment adopted in these patients. Figure S3 shows overall and prostate cancer-specific survival by main treatment adopted in these patients.

Radical prostatectomy

RP was carried out in 3212 patients (see Table S2, supporting information). Overall, 96.2% of RP patients had radical prostatectomy through the retropubic approach, and 89% had an open procedure. Concerning neurovascular bundle preservation, 70.4% of the patients received RP without nerve preservation. Lymph node dissection was carried out in 91% of the patients with mainly limited obturator lymph node dissection (71.6%).